

Accurate calling of KIAA1549 BRAF fusions from DNA of human brain tumours using methylation array based copy number and gene panel sequencing data

Damian Stichel, Daniel Schrimpf, Philipp Sievers, Annekathrin Reinhardt, Abigail K. Suwala, Martin Sill, David E. Reuss, Andrey Korshunov, Belén M. Casalini, Alexander C. Sommerkamp, Jonas Ecker, Florian Selt, Dominik Sturm, Astrid Gnekow, Arend Koch, Michèle Simon, Pablo Hernáiz Driever, Ulrich Schüller, David Capper, Cornelis M. Tilburg, Olaf Witt, Till Milde, Stefan M. Pfister, David T. W. Jones, Andreas Deimling, Felix Sahm, Annika K. Wefers

Angaben zur Veröffentlichung / Publication details:



Stichel, Damian, Daniel Schrimpf, Philipp Sievers, Annekathrin Reinhardt, Abigail K. Suwala, Martin Sill, David E. Reuss, et al. 2021. "Accurate calling of KIAA1549 BRAF fusions from DNA of human brain tumours using methylation array based copy number and gene panel sequencing data." *Neuropathology and Applied Neurobiology* 47 (3): 406–14.
<https://doi.org/10.1111/nan.12683>.

Nutzungsbedingungen / Terms of use:

CC BY 4.0



Accurate calling of *KIAA1549-BRAF* fusions from DNA of human brain tumours using methylation array-based copy number and gene panel sequencing data

Damian Stichel^{1,2} | Daniel Schrimpf^{1,2} | Philipp Sievers^{1,2} | Annekathrin Reinhardt^{1,2} | Abigail K. Suwala^{1,2} | Martin Sill^{3,4} | David E. Reuss^{1,2} | Andrey Korshunov^{1,2,3} | Belén M. Casalini^{1,2} | Alexander C. Sommerkamp^{3,5,6} | Jonas Ecker^{3,7,8} | Florian Selt^{3,7,8} | Dominik Sturm^{3,5,7} | Astrid Gnekow⁹ | Arend Koch^{10,11} | Michèle Simon¹² | Pablo Hernáiz Driever¹² | Ulrich Schüller^{13,14,15} | David Capper^{10,11} | Cornelis M. van Tilburg^{3,7,8} | Olaf Witt^{3,7,8} | Till Milde^{3,7,8} | Stefan M. Pfister^{3,4,7} | David T. W. Jones^{3,5} | Andreas von Deimling^{1,2} | Felix Sahm^{1,2,3}  | Annika K. Wefers^{1,2,3,13,14,15} 

¹Department of Neuropathology, Institute of Pathology, Heidelberg University Hospital, Heidelberg, Germany

²Clinical Cooperation Unit Neuropathology, German Consortium for Translational Cancer Research (DKTK), German Cancer Research Center (DKFZ), Heidelberg, Germany

³Hopp Children's Cancer Center (KiTZ), Heidelberg, Germany

⁴Division of Pediatric Neurooncology, German Cancer Consortium (DKTK), German Cancer Research Center (DKFZ), Heidelberg, Germany

⁵Pediatric Glioma Research Group, German Cancer Research Center (DKFZ), Heidelberg, Germany

⁶Faculty of Biosciences, Heidelberg University, Heidelberg, Germany

⁷Department of Pediatric Oncology, Hematology, Immunology and Pulmonology, Heidelberg University Hospital, Heidelberg, Germany

⁸Clinical Cooperation Unit Pediatric Oncology, German Cancer Research Center (DKFZ) and German Cancer Consortium (DKTK), Heidelberg, Germany

⁹Swabian Children's Cancer Center, University Hospital Augsburg, Augsburg, Germany

¹⁰Department of Neuropathology, Charité-Universitätsmedizin Berlin, Corporate member of Freie Universität Berlin, Humboldt-Universität zu Berlin and Berlin Institute of Health, Berlin, Germany

¹¹German Cancer Consortium (DKTK, Partner Site Berlin, German Cancer Research Center (DKFZ, Heidelberg, Germany

¹²Department of Pediatric Oncology/Hematology and Stem Cell Transplantation, Charité-Universitätsmedizin Berlin, Corporate member of Freie Universität Berlin, Humboldt-Universität zu Berlin and Berlin Institute of Health, Berlin, Germany

¹³Institute of Neuropathology, University Medical Center Hamburg-Eppendorf, Hamburg, Germany

¹⁴Department of Pediatric Hematology and Oncology, University Medical Center Hamburg-Eppendorf, Hamburg, Germany

¹⁵Research Institute Children's Cancer Center Hamburg, Hamburg, Germany

Correspondence

Damian Stichel, Department of Neuropathology, Heidelberg University Hospital, Im Neuenheimer Feld 224, 69120 Heidelberg, Germany.
Email: damian.stichel@med.uni-heidelberg.de

Annika K. Wefers, Institute of Neuropathology, University Medical

Abstract

Aims: *KIAA1549-BRAF* fusions occur in certain brain tumours and provide druggable targets due to a constitutive activation of the MAP-kinase pathway. We introduce workflows for calling the *KIAA1549-BRAF* fusion from DNA methylation array-derived copy number as well as DNA panel sequencing data.

This is an open access article under the terms of the Creative Commons Attribution License, which permits use, distribution and reproduction in any medium, provided the original work is properly cited.

© 2020 The Authors. Neuropathology and Applied Neurobiology published by John Wiley & Sons Ltd on behalf of British Neuropathological Society.

Center Hamburg-Eppendorf,
Martinistraße 52, 20246 Hamburg,
Germany.
Email: a.wefers@uke.de

Funding information

Medical Faculty of Heidelberg, Grant/
Award Number: Physician Scientist-
Program; Else Kröner-Fresenius Stiftung,
Grant/Award Number: Else Kröner
Excellence Program; The Brain Tumour
Charity, UK, Grant/Award Number:
Everest Centre for Low-grade Paediatric
Brain Tumours

Methods: Copy number profiles were analysed by automated screening and visual verification of a tandem duplication on chromosome 7q34, indicative of the *KIAA1549-BRAF* fusion. Pilocytic astrocytomas of the ICGC cohort with known fusion status were used for validation. *KIAA1549-BRAF* fusions were called from DNA panel sequencing data using the fusion callers Manta, Arriba with modified filtering criteria and deFuse. We screened DNA methylation and panel sequencing data of 7790 specimens from brain tumour and sarcoma entities.

Results: We identified the fusion in 337 brain tumours with both DNA methylation and panel sequencing data. Among these, we detected the fusion from copy number data in 84% and from DNA panel sequencing data in more than 90% using Arriba with modified filters. While in 74% the *KIAA1549-BRAF* fusion was detected from both methylation array-derived copy number and panel sequencing data, in 9% it was detected from copy number data only and in 16% from panel data only. The fusion was almost exclusively found in pilocytic astrocytomas, diffuse leptomeningeal glioneuronal tumours and high-grade astrocytomas with piloid features.

Conclusions: The *KIAA1549-BRAF* fusion can be reliably detected from either DNA methylation array or DNA panel data. The use of both methods is recommended for the most sensitive detection of this diagnostically and therapeutically important marker.

KEYWORDS

Arriba, DNA methylation, DNA panel sequencing, gene fusion, *KIAA1549-BRAF*, pilocytic astrocytoma

INTRODUCTION

A fusion of the genes *KIAA1549* and *BRAF*, generated through a focal tandem duplication on 7q34, causes constitutive activation of the mitogen-activated protein kinase (MAPK) pathway [1]. It initiates cell growth, migration, differentiation and survival, and plays a crucial role in tumour development [2]. Hence, MEK inhibitors may be considered as a therapeutic option in the presence of a *KIAA1549-BRAF* fusion [3, 4]. The *KIAA1549-BRAF* fusion is the most common genetic alteration in pilocytic astrocytoma [1], but it also occurs in other central nervous system (CNS) tumours such as diffuse leptomeningeal glioneuronal tumour (DLGNT) [5, 6] and high-grade astrocytoma with piloid features [7].

Several variants of the *KIAA1549-BRAF* fusion exist, with fusions of exons 16:9 and 15:9 being the most frequent events [1, 8]. Calling of *KIAA1549-BRAF* fusions is commonly performed using fluorescence *in situ* hybridization (FISH) or targeted RT-PCR [1, 9–11]. However, these techniques may miss some variants [12]. While RNA sequencing is currently becoming the gold standard for detection of gene fusions and is increasingly used in diagnostic settings [13–15], it is still not universally available and may be challenging from formalin-fixed paraffin-embedded samples (FFPE).

DNA methylation profiling is becoming more widely used in routine diagnostics of brain tumours [16]. Copy number profiles calculated from DNA methylation data may be used for the detection of a focal copy number gain on 7q34, resulting from the tandem duplication generating the *KIAA1549-BRAF* fusion. Visual calling of this gain has

been done in some studies [6, 7, 16]. However, so far it has not been validated how reliably this gain can be detected, and how closely such an event called visually correlates with the presence of this fusion. Furthermore, prior to a visual inspection, an automated algorithm to detect focal gains suggesting a *KIAA1549-BRAF* fusion might be helpful for a pre-evaluation for diagnostic purposes, or when screening larger cohorts as recently exemplified for *YAP1* fusions [17].

In addition to DNA methylation profiling, DNA panel sequencing from FFPE tissue is also becoming more widely available in routine diagnostics. If intronic sequences of potential fusion partners such as *KIAA1549* and *BRAF* are covered in a gene panel, it may be used for gene fusion detection. However, few data regarding how reliably the *KIAA1549-BRAF* fusion can be detected from DNA panel data and which algorithms are suitable for the analysis are available.

MATERIALS AND METHODS

Data generation

DNA methylation analysis

DNA was processed using the Illumina HumanMethylation450 or EPIC BeadChip array as previously described [18]. The data were analysed with the DNA methylation-based brain tumour classifier [18]. Samples were regarded classifiable to a DNA methylation class if the calibrated classifier score was ≥ 0.9 . A detailed description of

the methylation classes is outlined under <https://www.molecularneuropathology.org>. The same analysis was done using the sarcoma classifier (<https://www.molecularsarcomapathology.org>; Koelsche C *et al.*, accepted for publication).

DNA panel sequencing

Gene panel sequencing from FFPE samples was performed and data were processed as previously described.[19] The applied brain tumour gene panel covers intronic regions of the genes *KIAA1549* and *BRAF* (see Table S1 for details on all covered regions on chromosome 7).

RNA sequencing

RNA sequencing of formalin-fixed paraffin-embedded tissue was performed as previously described [14]. These data were used as additional validation.

RT-PCR

RNA was extracted from FFPE tissue with the Maxwell 16 LEV RNA FFPE Kit (Promega, Fitchburg, WI, USA) according to the manufacturer's instructions. cDNA was obtained using the SuperScript III Reverse Transcriptase (Thermo Fisher). PCRs for the most common fusion transcripts of *KIAA1549* ex. 15 – *BRAF* ex. 9, *KIAA1549* ex. 16 – *BRAF* ex. 9 and *KIAA1549* ex. 16 – *BRAF* ex. 11 were then done as described previously [9].

Calling of the *KIAA1549-BRAF* fusion

Calling of the *KIAA1549-BRAF* fusion by visual and automated inspection of copy number profiles calculated from DNA methylation array data

Copy number profiles were computed from the methylation data using the R package *conumee* [20]. Visual inspection indicated a *KIAA1549-BRAF* fusion in the copy number profiles if a narrow gain of the 7q34 region, representing the duplication, was present. In the automated analysis, evidence of the *KIAA1549-BRAF* fusion in the copy number profile was given if the median intensity of the probes on 7q34, which are involved in the duplication region (range: 7:138.500.000–7:140.500.000, GRCh37), was 0.1 higher than the median intensity of all probes on the whole chromosome 7q, as well as 0.07 higher than the median intensity of all probes on 7q33 and 0.07 higher than the median intensity of all probes on 7q35. To avoid false positives, the fusion was not called automatically if one arm of chromosome 7 was split into 10 or more segments by the circular binary segmentation algorithm implemented in the R package *DNAcopy* [21]. This may occur in cases with low DNA quality or complex rearrangements such as chromothripsis on chromosome 7 [22].

Calling of the *KIAA1549-BRAF* fusion from DNA panel sequencing data

To call *KIAA1549-BRAF* fusions from fastq files derived from DNA panel sequencing, we used the independent tools Manta [23] (version 1.6.0; with parameter `--rna`, all calls with "PASS" in the column "filter" kept), deFuse [24] with standard settings and Arriba (<https://github.com/suhrig/Arriba>, version 1.2.0 with STAR aligner [25] version 2.6.1e), initially with standard settings. In addition, we searched for *KIAA1549-BRAF* fusions in the 'discarded' output of the Arriba analysis for all cases for which no *KIAA1549-BRAF* fusion was indicated by Arriba in the main output file. The standard settings of Arriba were developed for analysis of RNA sequencing data. Thus, all fusions with no supporting reads overlapping an exon are automatically discarded. As the breakpoints on the DNA level are almost exclusively in intronic sequences, we retrieved all *KIAA1549-BRAF* fusions from the original discarded output of Arriba that had been discarded by the filters 'intronic', 'mismatches' or 'mismappers', provided that at least two supporting reads were present. If more than one alignment variant of the *KIAA1549-BRAF* fusion was found in similar positions in the discarded output, we chose the one with the highest number of split reads.

Calling of the *KIAA1549-BRAF* fusion from RNA sequencing data

We used the independent tools deFuse [24] and Arriba (<https://github.com/suhrig/Arriba>, version 1.2.0 with STAR aligner [25] version 2.6.1e) with standard settings.

Sample selection

The cohort was compiled from archival tissue for which ethical approval for research use was granted by local regulations.

Further data analysis

All further analyses were performed in R,[26] version 3.4.4. Plots of Figure S3 were created using the script 'draw_fusions.R' in R, available at <https://github.com/suhrig/Arriba>.

RESULTS

Automated and visual calling of a gain of 7q34, indicative of the *KIAA1549-BRAF* fusion, from copy number profiles calculated from DNA methylation data show a high correlation

To investigate whether an automated analysis of copy number profiles from DNA methylation data can be reliably used for a

screening of a 7q34 duplication, we defined criteria for an automated analysis (see methods). We screened DNA methylation data from 19,532 samples (13,617 FFPE, 5,915 fresh frozen), classifiable with the brain tumour classifier,[18] for a gain of 7q34. A gain of 7q34 was detected in 732/19,532 (4%; 545 FFPE, 187 fresh frozen) with the automated analysis. An example of a copy number profile

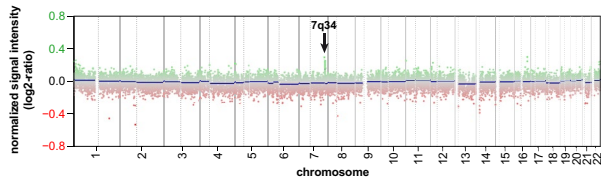


FIGURE 1 Exemplary copy number profile from a pilocytic astrocytoma WHO grade I with a KIAA1549 ex. 16-BRAF ex. 9 fusion showing a 7q34 gain (arrow) caused by the tandem duplication of KIAA1549 and BRAF on the chromosome 7q34 locus

showing the typical gain is depicted in Figure 1. All cases with evidence of a fusion were independently re-analysed visually by an experienced neuropathologist. Comparison to the visual analysis showed accordance in the vast majority of cases (673/732, 92%; Figure 2A). The majority of discrepancies in cases with a gain in the automated analysis related to low DNA quality resulting in noisy copy number profiles (33/732 cases (5%) scored 'not evaluable', 26/732 cases (4%) 'possible gain' in the visual analysis).

After establishing a protocol for analysis of DNA panel data for the KIAA1549-BRAF fusion (see below), we repeated this analysis for all cases with FFPE material for which DNA panel data were available, and for which the KIAA1549-BRAF fusion was detected either by visual calling from copy number plots derived from DNA methylation data, independent of the classifier scores, or from DNA or RNA sequencing data, that is, cases in which the KIAA1549-BRAF fusion was detected with at least one method used ($n = 354$, Table S2; Figure S1). Again, there was concordance in the majority of cases

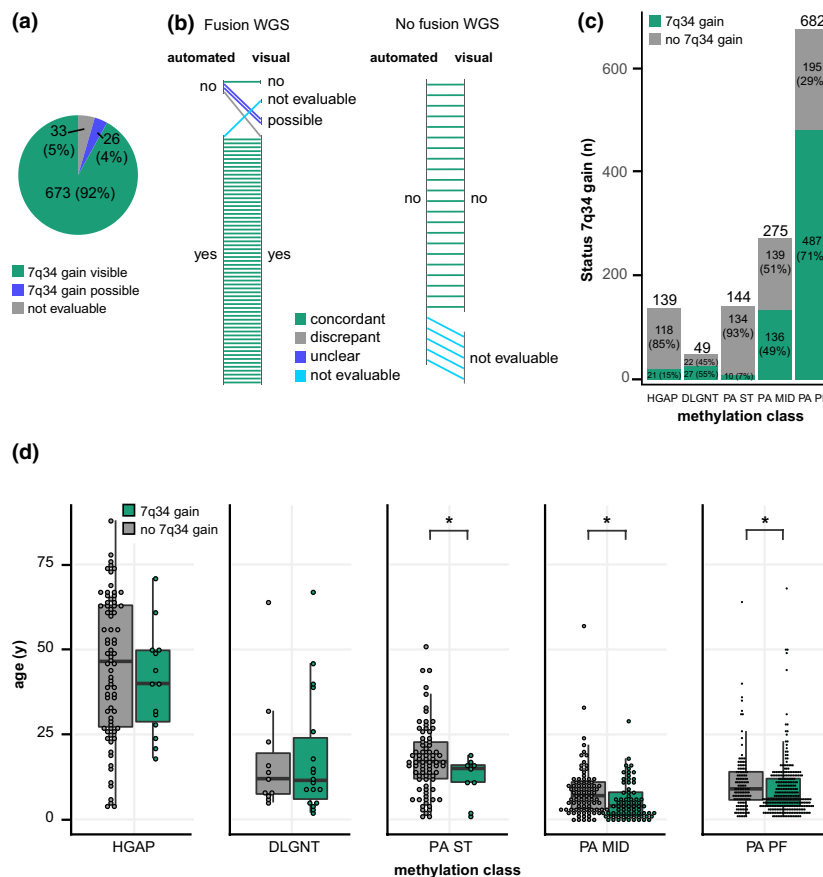


FIGURE 2 A 7q34 gain, indicative of the KIAA1549-BRAF fusion, can be detected from copy number profiles calculated from DNA methylation arrays by visual and automated analyses. (A) Assessment of a 7q34 gain by visual analysis for all cases for which a 7q34 gain was detected with an automated analysis ($n = 732$). (B) Automated and visual analysis of copy number plots from pilocytic astrocytomas of the ICGC cohort for a 7q34 gain (Table S3, $n = 95$). KIAA1549-BRAF status known for all samples from whole-genome sequencing (WGS). Left: Cases with fusion proven by WGS, right: cases without fusion. (C) Frequency of a 7q34 gain in samples classified as methylation class high-grade astrocytoma with piloid features (HGAP), methylation class diffuse leptomeningeal glioneuronal tumour (DLGNT), methylation class low-grade glioma, subclass hemispheric pilocytic astrocytoma and ganglioglioma (PA ST), methylation class low grade glioma, subclass midline pilocytic astrocytoma (PA MID) and methylation class low-grade glioma, subclass posterior fossa pilocytic astrocytoma (PA PF). Automated analysis (total $n = 1290$ samples). (D) Age distribution of patients with tumours with and without 7q34 gain. Methylation classes as in C ($n = 800$). * $p < 0.05$

($n = 301/354$, 85%) and we did not observe any case that was fusion positive with the automated analysis but clearly fusion negative upon visual inspection. In only 7/343 cases (2%), a *KIAA1549-BRAF* fusion was detected by visual but not by automated analysis.

For validation purposes, we analysed a published ICGC dataset of 95 pilocytic astrocytomas with known *KIAA1549-BRAF* status derived from whole-genome sequencing (WGS) [27] ($n = 68$ fusion positive, $n = 27$ fusion negative). Both with the automated analysis and an independent visual analysis, we received a specificity of 100% and a sensitivity of 96% in this cohort as compared to WGS data (Figure 2B, Table S3). The results of the automated and visual analysis differed in nine samples (only one clearly discrepant; two "possible" and six "not evaluable" in the visual analysis).

In summary, we found that a gain of 7q34, indicative of a *KIAA1549-BRAF* fusion, can be detected from DNA methylation data with high sensitivity and specificity. The automated calling of a gain of 7q34 shows a high agreement with a visual analysis.

A gain of 7q34 is almost exclusively detected in a few glioma entities known to harbour *KIAA1549-BRAF* fusions

To determine in which tumour entities a gain of 7q34, indicative of a *KIAA1549-BRAF* fusion, occurs, we analysed to which methylation classes (MC) of the brain tumour classifier the 673 tumours belonged for which a gain was detected both with the automated and visual analysis (Table S4). As expected, most cases were assigned to methylation classes of pilocytic astrocytoma (PA; $n = 616$), diffuse leptomeningeal glioneuronal tumour (DLGNT; $n = 27$) and high-grade astrocytoma with piloid features (HGAP, previously referred to as anaplastic astrocytoma with piloid features, or anaplastic PA; $n = 21$). Four positive cases originally classified as glioblastoma, IDH wild type, subclass midline most likely also represent DLGNTs according to their copy number profiles and a t-distributed stochastic neighbour embedding analysis (t-SNE). One case was classified as desmoplastic infantile astrocytoma/ganglioglioma. Single cases belonged to methylation classes of control tissue that may contain, for example, pilocytic astrocytomas with a low tumour cell content. Only 3/673 cases (0.4%) were assigned to methylation classes for which the presence of a *KIAA1549-BRAF* fusion is unlikely (one case each in methylation class glioblastoma, IDH wild type, subclass mesenchymal; methylation class IDH-mutant glioma, subclass high-grade astrocytoma; methylation class CNS Ewing sarcoma family tumour with CIC alteration). In two of these cases, the gain was not entirely prototypical. For the third case, no material was left to confirm or exclude the presence of the fusion. In summary, all cases but one (1/673, 0.1%) with a gain of 7q34 were assigned to methylation classes of entities known to harbour the *KIAA1549-BRAF* fusion, that is, mainly pilocytic astrocytoma but also DLGNT and HGAP. With the automated analysis alone, a small number of additional cases with hints of a *KIAA1549-BRAF* fusion assigned to different methylation classes were detected.

However, many of these were scored "not evaluable" with a visual analysis (Figure 2A; Table S4).

Additionally, we analysed methylation data of $n = 3311$ tumours that were classifiable with the sarcoma classifier (Koelsche C et al., accepted for publication) but not the brain tumour classifier, as the *KIAA1549-BRAF* fusion has not been described in sarcomas. The automated analysis predicted a gain of 7q34 in only 0.4% of cases ($n = 14/3311$; Table S5). Most of these cases were related to an increased signal-to-noise ratio and scored 'not evaluable' ($n = 9/14$, 64%) or 'possible' ($n = 3/14$, 21%) in the visual analysis. Only in two cases was a gain confirmed in the visual analysis. However, one of these cases was a pilocytic astrocytoma that was misclassified by the sarcoma classifier due to a high content of inflammatory cells. The other one was a chondrosarcoma with a 7q34 gain that was not entirely prototypical and, as expected, no *KIAA1549-BRAF* fusion was detected by RNA sequencing.

Thus, we conclude that a gain of 7q34, indicative of a *KIAA1549-BRAF* fusion, in copy number profiles calculated from DNA methylation data is almost exclusively found in the few gliomas/glioneuronal tumours known to harbour *KIAA1549-BRAF* fusions.

The frequency and age distribution of 7q34 gain vary in different methylation classes of glial/glioneuronal tumours

For all methylation classes with frequent gain of 7q34, that is, methylation classes of PA, DLGNT and HGAP, we calculated the percentage of tumours with a gain of 7q34 in an automated analysis. In line with earlier publications, a gain was detected in 71% of pilocytic astrocytomas of the posterior fossa (487/682; Figure 2C) and about half of pilocytic astrocytomas of the midline (136/275; 49%) but was rare in supratentorial tumours (7%; 10/144). Also, the gain was detected in about half of DLGNT (27/49; 55%) and in 15% of HGAP (21/139). In HGAP and DLGNT, the 7q34 gain occurs in all age groups, whereas in pilocytic astrocytomas, it is significantly more frequent in younger children (posterior fossa mean age fusion positive: 8.6 years, mean age fusion negative: 10.7 years, $p = 0.03$, t-test; midline 5.4 vs. 8.4 years, $p = 0.05$; supratentorial 12.0 vs. 17.7 years, $p = 0.03$; no significant difference in HGAP (39.9 vs. 44.9 years, $p = 0.3$) and DLGNT (18.5 vs. 17.7 years, $p = 0.9$); Figure 2D).

The *KIAA1549-BRAF* fusion can be reliably detected from DNA panel sequencing data

To evaluate whether the *KIAA1549-BRAF* fusion can be reliably identified from DNA panel data, we pre-selected cases from our database for which the fusion had been called in copy number analyses from DNA methylation data and for which panel sequencing data were available ($n = 282$, all FFPE). In this set, Arriba with modified filter settings detected the *KIAA1549-BRAF* fusion from panel sequencing data in 89% of copy number-positive cases (251/282) as

opposed to only 10% with the unmodified Arriba (27/282; data not shown).

Next, all panel sequencing data available were analysed for the presence of this fusion. Cases for which the fusion had been called either in copy number analyses from DNA methylation data or in sequencing data with one or several of the fusion callers deFuse, Manta or Arriba, and for which panel sequencing data were available, were selected, that is, all cases with evidence of a KIAA1549-BRAF fusion ($n = 348$, Table S2; in addition, the table contains cases with RNA-Seq data). deFuse detected the KIAA1549-BRAF fusion in about 55% of cases ($n = 191/348$; Figure 3; Table S2) while Manta detected it in 72% of cases ($n = 249/348$). We achieved the highest detection rate of 90% with Arriba with modified filter settings ($n = 314/348$; Figure 3; Table S2). Since only in few cases the fusion was detected with Manta and/or deFuse but not with Arriba, use of all three fusion callers combined only slightly increased the overall detection rate from 90% with Arriba only to a total of 94% ($n = 328/348$; Figure 3). Thus, in this setting, Arriba with modified filter settings is well suited to detect the KIAA1549-BRAF fusion. Figure S3 illustrates an exemplary fusion.

To check whether these results are specific, we assigned all classifiable cases with DNA methylation data to methylation classes using the brain tumour classifier. The fusion was again only detected in different methylation classes of pilocytic astrocytoma, DLGNT, HGAP and control tissue, suggestive of a low tumour cell content

(integrated diagnoses in Table S2). Thus, we conclude that the algorithm is specific.

In summary, the analysis of DNA panel sequencing data is well suited to detect the KIAA1549-BRAF fusion in a diagnostic setting.

The KIAA1549-BRAF fusion is detected in most cases by both copy number analyses from DNA methylation data and by fusion calling from DNA panel data

To evaluate whether calling of the KIAA1549-BRAF fusion from DNA methylation data or from DNA panel sequencing data is more sensitive, we selected cases for which both DNA methylation data and data from DNA panel sequencing were available, and in which the KIAA1549-BRAF fusion was detected with at least one of the methods used. Among these, we detected the fusion from DNA methylation data in 84% of the cases by visual analysis (Fig. S2). From DNA panel sequencing data, the fusion was again detected in more than 90% using Arriba with modified filters (304/337), and in only a further 4% when adding deFuse and Manta (13/337). Further comparisons of DNA methylation analyses and panel sequencing analyses with the modified Arriba indicate that in the vast majority of cases, the KIAA1549-BRAF fusion was detected with methylation and panel analyses ($n = 251/337$; 74%; Fig. S2). However, in 9% (31/337), there was only evidence of the KIAA1549-BRAF fusion from copy number data while in 16% (53/337), the fusion was detected only from DNA panel sequencing data.

For an additional validation, we selected all cases from our database for which RNA sequencing data from FFPE tissue was available, and for which the KIAA1549-BRAF fusion was detected either by visual calling from copy number plots derived from DNA methylation data or from any type of sequencing data ($n = 30$; Table S2). In total, we screened RNA sequencing data from 1462 samples of various brain tumour and sarcoma entities with deFuse and Arriba for a KIAA1549-BRAF fusion. For one of the selected samples, only RNA sequencing data were available while for all other cases, DNA methylation data and for 23 cases also DNA panel data were available.

As published earlier [14], Arriba was much more sensitive than deFuse in the detection of gene fusions from RNA-sequencing data (Arriba 87% (26/30) vs. deFuse 30% (9/30), Fig. S4). An exemplary gene fusion called is illustrated in Figure S3b.

We then compared the detection of the KIAA1549-BRAF fusion in these cases by RNA sequencing to the detection from copy number profiles or DNA panel sequencing. For 25/26 cases with proven fusions from RNA sequencing data, methylation data were available. In 19 of these cases (76%), a gain of 7q34 was detected in a visual evaluation of the copy number profiles. In 4/25 cases (16%), a gain was possible while in two cases, it was not detected (2/25, 8%). In 19/21 cases (90%) with proven fusions from RNA sequencing data and with additional DNA panel data, the fusion was detected from DNA panel data with Arriba. In 14/23 cases (61%) for which DNA methylation and both DNA panel and RNA

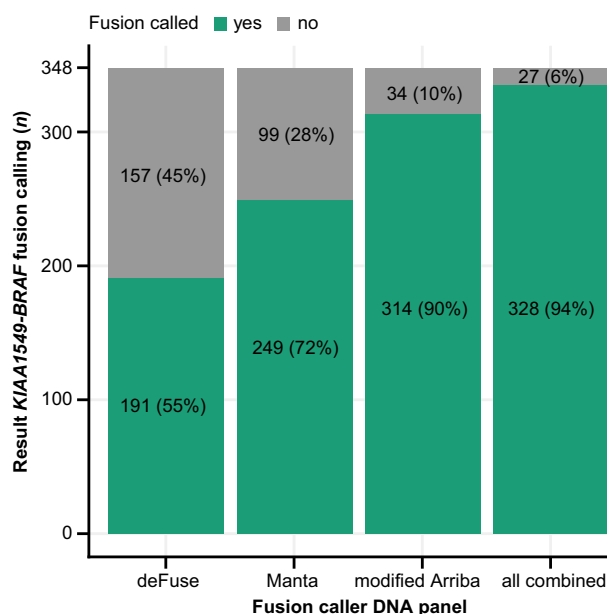


FIGURE 3 The KIAA1549-BRAF fusion can be reliably detected with DNA panel sequencing. Number of called fusions with the following fusion callers (from left to right): deFuse, Manta and Arriba with modified filter settings, combination of the three tools. Included were all cases with panel sequencing data in which evidence for a KIAA1549-BRAF fusion was found either in copy number profiles from DNA methylation data or in sequencing data ($n = 348$ cases). A version of this figure including RNA sequencing data is depicted in Figure S4

sequencing data were available, the fusion was detected with all methods used.

In 3/4 of the cases in which the *KIAA1549-BRAF* fusion was not detected by RNA sequencing, a gain of 7q34 was visible in the copy number profile. In two of these four cases (50%), the fusion was also detected from panel sequencing data. The presence of the fusion in these four cases could be confirmed by identifying a split read in the RNA fastq files using the grep command as proposed in Panagopoulos, Gorunova [28]. Thus, compared to the RNA sequencing data as reference, in this set (588 samples with both DNA and RNA sequencing data analysed, 1129 samples with both RNA sequencing and methylation data analysed) our methods for calling the *KIAA1549-BRAF* fusion from methylation and panel data returned no false positives.

Even though the RNA dataset is comparatively small, these data show again that while *KIAA1549-BRAF* fusions are detected with several methods in most cases, they may be missed in individual cases when using only one method.

Finally, we did exemplary RT-PCRs for *KIAA1549-BRAF* fusions of exons 15 and 9, 16:9 and 16:11 to additionally confirm the results from DNA panel sequencing and RNA sequencing. As expected, fusions of exons 15–9 (two samples) and 16–9 (five samples) were detected by RT-PCR, whereas a fusion of exons 15 and 11 was missed (two samples; data not shown). In addition, we compared the data from whole-genome sequencing and copy number profiles from DNA methylation data of the ICGC validation cohort to the results of FISH-analyses and RT-PCRs of a subset. Results from the copy number analyses are well in line with those from exemplary FISH analyses and RT-PCR (Fig. S5). These data confirm that DNA panel sequencing and DNA methylation analyses are well suited to detect *KIAA1549-BRAF* fusions, and that even rare fusions may be discovered by DNA panel sequencing.

DISCUSSION

In this study, we compared the performance of different approaches for calling the *KIAA1549-BRAF* fusion from copy number data obtained with DNA methylation arrays and DNA panel sequencing data across a large cohort of brain tumour and sarcoma samples. We find that the *KIAA1549-BRAF* fusion can be reliably detected both from methylation array data and DNA panel sequencing data. Clinically, this is relevant both as a diagnostic/prognostic as well as a therapeutic marker, as patients with tumours harbouring a *KIAA1549-BRAF* fusion may be treated with MEK inhibitors [4].

The techniques most widely used for the detection of the *KIAA1549-BRAF* fusion are FISH analysis and RT-PCR. While FISH analysis depends on tissue integrity and thus may be technically challenging in some cases, RT-PCR approaches only cover the most common fusion combinations of *KIAA1549* and *BRAF*, that is, often exons 16:9, 15:9 and 16:11 [1, 12], and they also require suitable RNA. RNA sequencing on the other hand has a high sensitivity for the detection of all types of fusion transcripts, but it largely depends

on the RNA quality and thus may be challenging from some FFPE samples. Moreover, it is not yet widely available in a diagnostic context.

DNA methylation arrays, however, are becoming more and more widely used and can be used for computing a classifier diagnosis and a copy number profile at the same time [16, 18]. Visual analysis of the copy number profile has a high sensitivity for the detection of this fusion as validated with the ICGC dataset in our study. Moreover, the frequency of a gain of 7q34 and the age distribution in different methylation classes of pilocytic astrocytoma, DLGNT and HGAP were in line with the frequencies of *KIAA1549-BRAF* fusions reported earlier [6, 7, 9, 12]. The fusion was almost exclusively detected in these tumours, confirming the specificity of the method. Interestingly, in our large cohort, we never found a *KIAA1549-BRAF* fusion in gangliogliomas, for which the fusion has been described in single cases [29, 30], or dysembryoplastic neuroepithelial tumours.

For use in a clinical setting, we recommend confirming a *KIAA1549-BRAF* fusion as indicated by a gain of 7q34 with a second method, for example panel sequencing, in two scenarios. First, in cases in which a focal gain of 7q34 is not in line with the histological or molecular diagnosis, in order to rule out a different copy number alteration resembling a focal gain of 7q34 caused by a *KIAA1549-BRAF* tandem duplication. Second, in cases in which no 7q34 gain is detected or in which the gain is not the prototypical focal gain of 7q34, in which, however, the presence of a *BRAF* fusion might be expected. A gain of 7q34 may in exceptional cases be caused by a different *BRAF* fusion. This would also be clinically important, as it would also lead to a MAPK activation.

Our data furthermore indicate that automatic evaluation of the 7q34 tandem duplication from the copy number profiles shows a high concordance with visual inspection and is thus suitable for a fast automated screening of large datasets or an initial clinical evaluation of prospective cases. In the latter situation, however, a visual verification is recommended, especially in entities that have not previously been described to harbour *KIAA1549-BRAF* fusions. Based on these results, a screening of diagnostic cases or large datasets of DNA methylation data also for other relevant fusions resulting in copy number changes could be established.

Another technique that is becoming increasingly used in the diagnostic setting is DNA panel sequencing. The advantage of this technique is that if intronic sequences for certain gene fusions are included, it may be used to screen for mutations and gene fusions at the same time [19]. This is especially helpful for tumours such as supratentorial pilocytic astrocytomas that may harbour different alterations activating the MAPK pathway [12]. We show here that the algorithm Arriba is well suited to detect the *KIAA1549-BRAF* fusion from DNA panel data after adjusting the filter settings. While single extremely rare *KIAA1549-BRAF* fusions may be missed with DNA panel sequencing as it is not feasible to cover all intronic regions of the two genes, the vast majority is detected with the regions covered by the applied panel, that is, many more combinations than with RT-PCR. To some extent, the detection rate also depends on the DNA quality, although 93% of the fusions could be detected

with panel sequencing in our cohort, despite the DNA being derived from archival FFPE tissue. In comparison, panel sequencing performed slightly better than the analysis of DNA methylation-based copy number profiles (84%). While both have a high specificity and in the majority of cases use of one method is sufficient to detect the KIAA1549-BRAF fusion, a combination of both methods leads to a higher sensitivity. Copy number analyses may miss a gain of 7q34 due to a poor signal-to-noise ratio, and both copy number analyses and panel sequencing may miss the fusion due to a low tumour cell content or poor DNA quality. Thus, in cases without evidence of a KIAA1549-BRAF fusion with one method, in which, however, the presence of a KIAA1549-BRAF fusion is highly likely (e.g. pilocytic astrocytoma in the posterior fossa), use of a second method is recommended. In paediatric studies such as MNP2.0 and PTT2.0 [31], both methods are routinely used, increasing the likelihood of the detection of this fusion. The modified Arriba algorithm might in the future also be used for the detection of different fusion genes for which intronic sequences can be included in the DNA panel.

In conclusion, we show that the KIAA1549-BRAF fusion can be reliably detected both from copy number profiles generated from DNA methylation data and from DNA panel sequencing data in a diagnostic setting, and that this fusion is restricted to a handful of distinct molecular brain tumour classes.

Ethics approval and consent to participate

Tissue collection and processing as well as data collection were in compliance with local ethics regulations and approval.

ACKNOWLEDGEMENTS

We thank Katja Böhmer, Laura Dörner, Antje Habel, Lisa Kreinbihl, Ulrike Lass, Kerstin Lindenberg, Jochen Meyer and Hai Yen Nguyen for skilful technical assistance. We thank the Genomics and Proteomics Core Facility of the German Cancer Research Center (DKFZ) for the performance of DNA methylation analyses. A.K. Wefers was supported by the Physician Scientist-Program of the Medical Faculty of Heidelberg. D.T.W. Jones is supported by the Everest Centre for Low-grade Paediatric Brain Tumours (The Brain Tumour Charity, UK). F. Sahm is a fellow of the Else Kröner Excellence Program of the Else Kröner-Fresenius Stiftung (EKFS). Open access funding enabled and organized by ProjektDEAL.

CONFLICT OF INTEREST

D. Capper, D. T. W. Jones, M. Sill, A. von Deimling and S. M. Pfister declare that under the No. EP3067432A1 a patent was applied for a 'DNA-methylation based method for classifying tumour species'. C.M. van Tilburg participated at advisory boards of Novartis and Bayer.

AUTHOR CONTRIBUTIONS

A.K.W. and D.St. conceived the project, analysed the data and wrote the manuscript. All other authors were involved in the acquisition

or analysis of the data and contributed to the final version of the manuscript.

PEER REVIEW

The peer review history for this article is available at <https://publons.com/publon/10.1111/nan.12683>.

DATA AVAILABILITY STATEMENT

All processed data are included in this published article and it's supporting information files. Raw data are available upon request for collaborative research projects.

ORCID

Felix Sahm  <https://orcid.org/0000-0001-5441-1962>

Annika K. Wefers  <https://orcid.org/0000-0001-9394-8519>

REFERENCES

1. Jones DTW, Kocalkowski S, Liu L, et al. Tandem duplication producing a novel oncogenic BRAF fusion gene defines the majority of pilocytic astrocytomas. *Cancer Res*. 2008;68:8673.
2. Roberts PJ, Der CJ. Targeting the Raf-MEK-ERK mitogen-activated protein kinase cascade for the treatment of cancer. *Oncogene* 2007;26:3291-3310.
3. Schreck KC, Grossman SA, Pratilas CA. BRAF mutations and the utility of RAF and MEK inhibitors in primary brain tumors. *Cancers (Basel)* 2019;11.
4. Fangusaro J, Onar-Thomas A, Young Poussaint T, et al. Selumetinib in paediatric patients with BRAF-aberrant or neurofibromatosis type 1-associated recurrent, refractory, or progressive low-grade glioma: a multicentre, phase 2 trial. *Lancet Oncol*. 2019; 20:1011-1022.
5. Rodriguez FJ, Schniederjan MJ, Nicolaides T, Tihan T, Burger PC, Perry A. High rate of concurrent BRAF-KIAA1549 gene fusion and 1p deletion in disseminated oligodendroglioma-like leptomeningeal neoplasms (DOLN). *Acta Neuropathol*. 2015;129:609-610.
6. Deng MY, Sill M, Chiang J, et al. Molecularly defined diffuse leptomeningeal glioneuronal tumor (DLGNT) comprises two subgroups with distinct clinical and genetic features. *Acta Neuropathol*. 2018;136:239-253.
7. Reinhardt A, Stichel D, Schrimpf D, et al. Anaplastic astrocytoma with piloid features, a novel molecular class of IDH wildtype glioma with recurrent MAPK pathway, CDKN2A/B and ATRX alterations. *Acta Neuropathol*. 2018;136:273-291.
8. Tatevossian RG, Lawson ARJ, Forshaw T, Hindley GFL, Ellison DW, Sheer D. MAPK pathway activation and the origins of pediatric low-grade astrocytomas. *J Cell Physiol*. 2010;222:509-514.
9. Hasselblatt M, Riesmeier B, Lechtape B, et al. BRAF-KIAA1549 fusion transcripts are less frequent in pilocytic astrocytomas diagnosed in adults. *Neuropathol Appl Neurobiol*. 2011;37:803-806.
10. Tian Y, Rich BE, Vena N, et al. Detection of KIAA1549-BRAF fusion transcripts in formalin-fixed paraffin-embedded pediatric low-grade gliomas. *J Mol Diagn*. 2011;13:669-677.
11. Cin H, Meyer C, Herr R, et al. Oncogenic FAM131B-BRAF fusion resulting from 7q34 deletion comprises an alternative mechanism of MAPK pathway activation in pilocytic astrocytoma. *Acta Neuropathol*. 2011;121:763-774.
12. Collins VP, Jones DTW, Giannini C. Pilocytic astrocytoma: pathology, molecular mechanisms and markers. *Acta Neuropathol*. 2015;129:775-788.
13. Byron SA, Van Keuren-Jensen KR, Engelthaler DM, Carpten JD, Craig DW. Translating RNA sequencing into clinical diagnostics: opportunities and challenges. *Nat Rev Genet*. 2016;17:257-271.

14. Stichel D, Schrimpf D, Casalini B, et al. Routine RNA sequencing of formalin-fixed paraffin-embedded specimens in neuropathology diagnostics identifies diagnostically and therapeutically relevant gene fusions. *Acta Neuropathol.* 2019;138:827-835.
15. Sommerkamp AC, Uhrig S, Stichel D, et al. An optimized workflow to improve reliability of detection of KIAA1549:BRAF fusions from RNA sequencing data. *Acta Neuropathol.* 2020;140(2):237-239.
16. Capper D, Stichel D, Sahm F, et al. Practical implementation of DNA methylation and copy-number-based CNS tumor diagnostics: the Heidelberg experience. *Acta Neuropathol.* 2018;136(2):181-210.
17. Sievers P, Chiang J, Schrimpf D, et al. YAP1-fusions in pediatric NF2-wildtype meningioma. *Acta Neuropathol.* 2019;139(1):215-218.
18. Capper D, Jones DTW, Sill M, et al. DNA methylation-based classification of central nervous system tumours. *Nature* 2018;555:469-474.
19. Sahm F, Schrimpf D, Jones DW, et al. Next-generation sequencing in routine brain tumor diagnostics enables an integrated diagnosis and identifies actionable targets. *Acta Neuropathol.* 2015;1-8.
20. Hovestadt V, Zapatka M, Conumee: Enhanced copy-number variation analysis using Illumina DNA methylation arrays. R package version 1.9.0.
21. Olshen AB, Venkatraman ES, Lucito R, Wigler M. Circular binary segmentation for the analysis of array-based DNA copy number data. *Biostatistics* 2004;5:557-572.
22. Cohen A, Sato M, Aldape K, et al. DNA copy number analysis of Grade II-III and Grade IV gliomas reveals differences in molecular ontogeny including chromothripsis associated with IDH mutation status. *Acta Neuropathol Commun.* 2015;3:34.
23. Chen X, Schulz-Trieglaff O, Shaw R, et al. Manta: rapid detection of structural variants and indels for germline and cancer sequencing applications. *Bioinformatics* 2016;32:1220-1222.
24. McPherson A, Hormozdiari F, Zayed A, et al. deFuse: An Algorithm for gene fusion discovery in tumor RNA-Seq Data. *PLoS Comp Biol.* 2011;7:e1001138.
25. Dobin A, Davis CA, Schlesinger F, et al. STAR: ultrafast universal RNA-seq aligner. *Bioinformatics* 2013;29:15-21.
26. R Development Core Team. *R: A language and environment for statistical computing.* Vienna, Austria: R Foundation for Statistical Computing, 2011.
27. Jones DTW, Hutter B, Jager N, et al. Recurrent somatic alterations of FGFR1 and NTRK2 in pilocytic astrocytoma. *Nat Genet.* 2013;45:927-932.
28. Panagopoulos I, Gorunova L, Bjerkehaugen B, Heim S. The, "Grep" Command But Not FusionMap, FusionFinder or ChimeraScan Captures the CIC-DUX4 Fusion Gene from Whole Transcriptome Sequencing Data on a Small Round Cell Tumor with t(4;19)(q35;q13). *PLoS One* 2014;9:e99439.
29. Zhang J, Wu G, Miller CP, et al. Jude children's research hospital-washington university pediatric cancer Genome P. Whole-genome sequencing identifies genetic alterations in pediatric low-grade gliomas. *Nat Genet.* 2013;45:602-612.
30. Pekmezci M, Villanueva-Meyer JE, Goode B, et al. The genetic landscape of ganglioglioma. *Acta Neuropathol Commun.* 2018;6:47.
31. Selt F, Deiß A, Korshunov A, et al. Pediatric targeted therapy: clinical feasibility of personalized diagnostics in children with relapsed and progressive tumors. *Brain Pathol.* 2016;26:506-516.

SUPPORTING INFORMATION

Additional supporting information may be found online in the Supporting Information section.

How to cite this article: Stichel D, Schrimpf D, Sievers P, et al. Accurate calling of KIAA1549-BRAF fusions from DNA of human brain tumours using methylation array-based copy number and gene panel sequencing data. *Neuropathol Appl Neurobiol.* 2021;47:406-414. <https://doi.org/10.1111/nan.12683>